Steel and Composite Structures, *Vol. 23, No. 1 (2017) 95-105*
DOI: https://doi.org/10.12989/scs.2017.23.1.095

Incremental dynamic analyses of concrete buildings reinforced with shape memory alloy

Masoud Mirtaheri *, Mehrshad Amini [a] and Hossein Khorshidi [b]

Department of Civil Engineering, K.N.Toosi University of Technology, No. 1346, ValiAsr-Street, Mirdamad Intersection, P.O. Box 15875-4416, Tehran, Iran

(Received May 20, 2016, Revised December 08, 2016, Accepted December 14, 2016)

Abstract. The use of superelastic shape memory alloys (SMAs) as reinforcements in concrete structures is gradually gaining interest among researchers. Because of different mechanical properties of SMAs compared to the regular steel bars, the use of SMAs as reinforcement in the concrete may change the response of structures under seismic loads. In this study, the effect of SMAs as reinforcement in concrete structures is analytically investigated for 3-, 6- and 8-story reinforced concrete (RC) buildings. For each concrete building, three different reinforcement details are considered: (1) steel reinforcement (Steel) only, (2) SMA bar used in the plastic hinge region of the beams and steel bar in other regions (Steel-SMA), and (3), beams fully reinforced with SMA bar (SMA) and steel bar in other regions. For each case, columns are reinforced with steel bar. Incremental Dynamic Analyses (IDA) are performed using ten different ground motion records to determine the seismic performance of Steel, Steel-SMA and SMA RC buildings. Then fragility curves for each type of RC building by using IDA results for IO, LS and CP performance levels are calculated. Results obtained from the analyses indicate that 3-story frames have approximately the same spectral acceleration corresponding with failure of frames, but in the cases of 6 and 8-story frames, the spectral acceleration is higher in frames equipped with steel reinforcements. Furthermore, the probability of fragility in all frames increases by the building height for all performance levels. Finally, economic evaluation of the three systems are compared.

Keywords: concrete structures; superelastic shape memory alloys; incremental dynamic analysis; fragility curves

1. Introduction

Buildings in high seismic regions are prone to severe damage and collapse during earthquakes due to large lateral deformations. In particular, beam-column elements in reinforced concrete (RC) structures are extremely vulnerable and are considered the weakest link in such a structural system (Alam *et al*. 2008). In conventional seismic design of RC structures, reinforcing bars are expected to yield in order to dissipate energy while undergoing permanent deformations of post-yield steel reinforcing bars and damage of unconfined concrete. Consequently, in the event of large-scale earthquake, severe damage of infrastructure occurs resulting in the collapse of buildings, closing of bridges, unattainable post-disaster rescue operations, and overall substantial economic losses (Alam *et al*. 2008). Smart systems used in infrastructures are able to change structural characteristics in response to external disturbances or unexpected strong loads against structural safety and serviceability. An important technology to achieve this goal is the development of smart materials that can be used in structures.

Shape Memory Alloys (SMAs) are unique materials that have the ability to undergo large deformation and return to a predetermined shape upon unloading or by heating (Alam *et al*. 2009). Therefore, it can be an ideal solution for the problem of permanent deformations in structures. SMAs are gradually gaining interest and increasing reported applications in various engineering fields (Alam *et al*. 2007). Despite there are many types of shape memory alloys, the nickel–titanium (NiTi) alloy is one of the most available and appropriate materials used in various engineering fields. This alloy is based on the equiatomic compound of nickel and titanium, and both have the properties of superelasticity, shape memory effect and large recoverable strain. Manufacture of NiTi alloys is not an easy task and many machining techniques can only be used with difficulty. This fact explains the reason for the elevated cost of such a system. Despite this disadvantages, the excellent mechanical properties of NiTi alloys have made them the most frequently used SMA material in commercial applications. The alloys have been exploited in mechanical and electromechanical control systems to provide, for example, a precise mechanical response to small and repeated temperature changes (Srinivasan and McFarland 2001). Shape memory alloys are also used in a wide range of medical and dental applications (Anson 1999). According to the unique properties of shape memory alloys, they are utilized in a wide range of structural engineering including seismic isolators, braced systems, energy dissipation devices (dampers), repair and retrofit and its application in concrete structures.

*Corresponding author, Associate Professor
E-mail: mmirtaheri@kntu.ac.ir
[a] M.Sc., E-mail: mehrshadamino@gmail.com
[b] M.Sc., E-mail: hossein.khorshidi@mail.kntu.ac.ir

http://www.techno-press.org/?journal=scs&subpage=6 ISSN: 1229-9367 (Print), 1598-6233 (Online)

Dolce and Cardone (2001) investigated the mechanical behavior of several SMAs for seismic applications through a large experimental program. Superelastic behavior of several NiTi wires subjected to tension, and dependence of mechanical properties on the temperature, loading frequency and number of cycles were studied. The result show that the mechanical behavior of SMA bars subjected to tension is independent from temperature changes. In addition, loading frequency seems to affect the behavior of SMAs only when passing from nearly static conditions (0.01 Hz) to high frequency (0.2 to 0.4 Hz) in seismic applications (Dolce and Cardone 2001). Ocel *et al*. (2004) evaluated the feasibility of a new class of partially restrained connections using shape memory alloys in Steel Beam-Column Connections. For the first time, Mo *et al*. (2004) proposed the concept of intelligent reinforced concrete (IRC). The martensitic wires were used, and distribution of strain within concrete was evaluated by electrical resistance of SMA wires. The SMA wires shrunk by electrical heating when the crack was created. Motahari *et al*. (2007) studied the implementation of SMA dampers for passive control of structures subjected to seismic excitations. The effectiveness of the implementation of SMA dampers in reduction of the residual deformations on the structure was presented even after very high ground motions. Abdulridha *et al*. (2010) investigated the use of SMA bars in plastic hinges of beams and concrete shear walls in an experimental comprehensive program. Beams with SMA bars showed a significant increase in recovery capacity of concrete cracks. Khaloo *et al*. (2010) numerically investigated the response of cantilevered reinforced concrete (RC) beams with smart bars (Superelastic Shape Memory Alloys) under static lateral loading, using Finite Element Method. It was found that by using SMA bars in RC beams, these materials tended to return to the previous state (zero strain), and so they reduced the permanent deformations. Omar (2011) evaluated the seismic behavior of steel frames with different SMA systems including diagonal bracing, nee bracing and the last one was which the SMA was used a connection at the plastic hinge regions of beams. It concluded that implementing the SMA connection system was more effective in controlling the reaction forces at the base frame than other bracing systems. Andrawes and DesRoches (2007) conducted a sensitivity analysis to examine the effect of variability of each parameter on the effectiveness of SMAs as restrainers for bridges and bracings for buildings. The outcomes of the studies showed that the slope of the SMAs hysteresis had similar effect on the structural response (less than 10% in average) regardless of the type of SMA application. Alvandi *et al*. (2014) proposed the combination of SMA and base isolation systems as the passive control system in the building and/or bridge structures. The efficiency and feasibility of the two mechanisms were also presented by few cases in point.

Seismic energy dissipation in reinforced concrete buildings is through yielding of steel bars and inelastic deformations. Although life safety is provided, deformations of reinforced concrete buildings lead to damages and economic losses. The seismic design of structures is based on performance. Therefore, performance base design method results in more ductility, resistance against damages and decrease of permanent deformations in members and structural systems. Shape memory alloys are materials that have the ability to recover their shape after undergoing large deformations through either heating or removal of load (Dolce and Cardone 2001). According to the mentioned unique characteristics of SMAs, they are used as reinforcements in concrete members to improve the seismic behavior of buildings. Shin and Andrawes (2010) investigated the uniaxial compression behavior of concrete confined using an innovative active confinement technique (Shape memory alloys). The results of the study showed that SMA spirals exhibited stable recovery stress under monotonic and cyclic loading. The amount of prestrain losses measured in the study was minimal and thus had no impact on the behavior of the confined cylinders. In this paper, the use of SMAs as reinforcement in reinforced concrete buildings is investigated. For this purpose, the building with specific geometric details is considered. Three 3D reinforced concrete building including 3, 6 and 8 stories designed by Alam *et al*. (2012) are considered. For each concrete building, three different reinforcement details are considered: (1) steel reinforcement (steel) only; (2) SMA bar used in the plastic hinge region of the beams and steel bar in other regions (Steel-SMA); and (3), beams fully reinforced with SMA bar (SMA) and steel bar in other regions. The complete description of assumptions and design methods were mentioned in Alam *et al*. (2012). Then, different 2D concrete frames in term of height and reinforcement details are selected from 3D models, and modeled using OpenSees software. Incremental dynamic analyses (IDA) are performed using an ensemble of ten earthquake records to determine seismic behavior of various reinforcement details in frames. In addition, Fragility curves for performance levels of concrete frames base on FEMA356 are obtained. In addition, all the three various systems are evaluated and compared in terms of economic aspect, and the best of the three options which considered both performance and economic considerations are recommended.

2. Properties of superelastic shape memory alloys

Metals are characterized by physical features such as tensile strength, malleability and conductivity or diffusivity (thermal or electricity). In the case of shape memory alloys, there are other unique features. Shape memory alloys are made of different metals like copper, zinc, aluminum, nickel, titanium, manganese and iron. These alloys are able to undergo strains up to a maximum of ten percent without residual strains (superelastic behavior). SMAs are in the unique categories of metals that have the ability to recover imposed deformations and permanent strains, and eventually return to its original shape. The behavior of shape memory of alloys is based on the phase transformation and crystal structure changes. SMAs have complex behavior influenced by temperature, sample size, loading frequency and number of cycles. Suitable energy dissipation capability, high resistance to fatigue and corro-

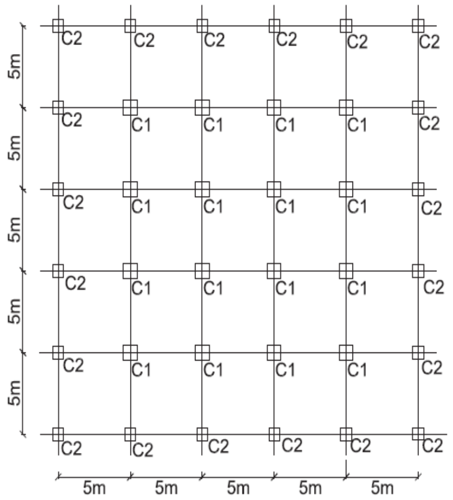

(a)

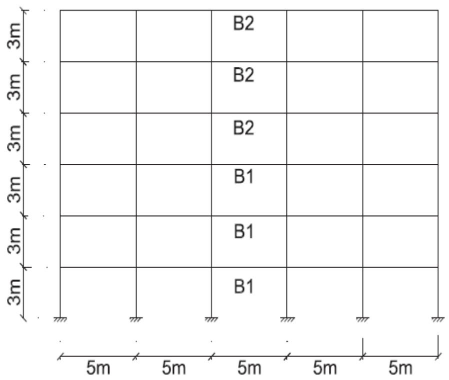

(b)

Fig. 1 Configuration of the typical six-story RC building (Alam *et al*. 2012): (a) Plan view; and (b) Elevation view

sion, high lifetime, no need for maintenance and possibility of eliminating residual strains by applying heating (shape memory behavior) are all the unique features of shape memory alloys. Contrary to the increase of various number of shape memory alloys, only two system including NiTi and copper-based alloys are used in the industry. NiTi compared to copper based alloys have greater recoverable strains (more than 8% against 4% in copper-based alloys). In addition, NiTi alloys are highly resistant to corrosion.

Table 1 Material Properties used in finite element analyses (Alam *et al*. 2012)

Material	Mechanical Property	Value
Concrete	Compressive strength (MPa)	35
	Tensile strength (MPa)	3.5
	Strain at peak stress (%)	0.2
Steel	Modulus of elasticity (MPa)	200.000
	Yield strength (MPa)	400
	Strain hardening parameter (%)	0.5
SMA	Modulus of elasticity (MPa)	60.000
	Austenite to martensite starting stress (MPa)	400
	Austenite to martensite finishing stress (MPa)	500
	Martensite to austenite starting stress (MPa)	300
	Martensite to austenite finishing stress (MPa)	100
	Super elastic plateau strain length (%)	6

Despite having excellent superelastic properties, can be expensive in the practice due to the high cost of Titanium, and because NiTi is hard to machine (Varela and Saiidi 2014).

3. Prototype building layout and design assumptions

In order to evaluate the effect of SMAs on structural response, three buildings including 3, 6 and 8 stories are considered (Alam *et al*. 2012). Each building hasfive bays in both directions with the same bay length of 5 m. Plan of all buildings are similar, and the height of each story is 3 m. The plan view of all buildings, and the elevation view of the 6-story building is shown in Figs. 1(a)-(b), respectively. Each building has three various types of bar in their beams, i.e., Steel, Steel-SMA and SMA as described in the previous section. It is notable that steel bars are used in the columns of three various types of building. Three Steel RC buildings of different stories have been analyzed as per NBCC and designed as moderately ductile moment resisting frames based on equivalent static force procedure according to CSA A23.3-04. Reinforcement details are based on CSA standards. The building is assumed to be located in the city of Vancouver in British Columbia, Canada. To calculate the design base shear, the same R_d and R_0 factors have been

Table 2 Beam reinforcement details (Alam *et al*. 2012)

Story ID	Beam ID	Size (mm)	Section ID (Fig. 2)					
			Section 1-1 Main reinforcement		Section 2-2 Main reinforcement		Section 3-3 Main reinforcement	
			Top (M)	Bottom (M)	Top (M)	Bottom (M)	Top (M)	Bottom (M)
3 Story building	B1	300×450	2-20	2-20	2-20	2-20	2-20	2-20
6 Story building	B1	300×500	3-25	4-25	3-25	4-25	5-25	4-20
	B2	300×500	2-20	2-20	2-20	3-20	2-20	3-20
8 Story building	B1	300×500	3-25	4-25	3-25	4-25	5-25	4-20
	B2	300×500	3-20	3-20	3-20	3-20	3-20	3-20

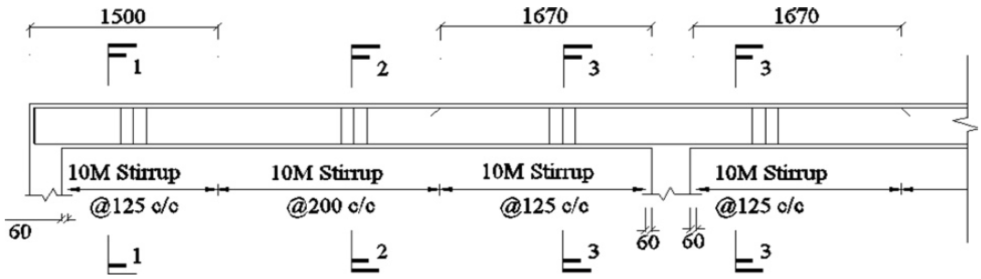

Fig. 2 Longitudinal section of beam reinforcement (typical) (Alam *et al*. 2012)

used for each frame type (Alam *et al*. 2012). Table 1 presents the material properties used for the design and implementation into thefinite element analyses. Table 2 represents the member sizes and reinforcement detailing of beams. Fig. 2 shows the reinforcement detailing of a typical beam where the section details are presented. Column sizes and its reinforcement details, and further information were mentioned in Alam *et al*. (2012).

3.1 Calculation of plastic hinge length

For concrete buildings with two different reinforcement details (SMA and Steel-SMA), bars used in the plastic hinge region of the beams. Plastic hinge zone is calculated using Eq. (1) based on Paulay and Priestley (1992), where l_p is plastic hinge length, f_{ye} is longitudinal steel yield stress and d_{bl} is diameter of longitudinal bar.

$$l_b = 0.08l + 0.022d_{bl\,f_{ye}} \geq 0.3d_{bl}f_{ye} \tag{1}$$

In addition, Pauli and Priestly have suggested that l_p be limited to the amount of 0.5d where d is section depth.

4. Analytical model assumptions

Modern earthquake engineering utilizes modelling and simulation to understand the behavior and performance of structural systems during earthquakes. Pacific Earthquake Research Center (PEER) has developed OpenSees software (Mazzoni *et al*. 2007) for research and application of simulation for structures and geotechnical systems. Although 3D models were developed typically for the probabilistic analysis of seismic demand, in this paper, the incremental dynamic analyses were performed on the 2D frames selected from each of the three-dimensional structures by using OpenSees software. The reason for this simplification are the decrease of time analysis regarding to the large number of time-consuming analyses, and reducing the size of structure in order to evaluate its behavior more accurately. The Beams and columns are modeled using nonlinear displacement beam-column elements with linear distributed plasticity. Nonlinear fiber elements are used to model all structural components. Figs. 3(a)-(b) represent the finite element meshing layout of beam-column elements. As shown in Fig. 3(a), each beam is divided into three sections with various reinforcement patterns. In addition, each two side sections are also divided into another element with the specific plastic hinge length (L_p). The plastic hinge length is calculated by Eq. (1). Seven integration points are considered to define cross section with integrated properties. As shown in Fig. 3(b), the fiber elements (20 × 20) is used to model the concrete core, and the fiber elements (20 × 6) is used to modeled the concrete cover of the elements 2, 3 and 4 of the beam. Generally, the use of displacement beam-column element would create major inaccuracies in the area where high-plasticity exists. Therefore, the authors increase the number of elements in the length of members where high plasticity is anticipated. Therefore, the fiber elements (30 × 30) is used to model the concrete core, and the fiber elements (30 × 9) is used to modeled the concrete cover of the elements 1 and 5 (plastic hinge length) of the beam. As mentioned in previous sections, 2D frames modeled by OpenSees software are obtained from the original 3D models. Therefore, it is necessary that the mass of structure is properly transferred from 3D to 2D model. In this way, period of structure, seismic loads caused by earthquake records and dynamic analyses are not undergone any changes. Thus, the mass of structural members, dead loads (500 Kg/m^2) and 20% of live loads (200 Kg/m^2) which belong to the middle frame are calculated for each story. Calculated masses are centralized modeled in end nodes of each column. Table 3 shows the value of masses for all various frames in 3D and 2D models. The value of 0.05 as Rayleigh Damping for 2D modes are considered.

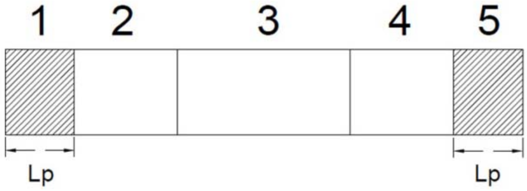

(a) Number of elements in beams

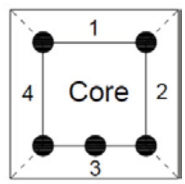

(b) Concrete core/cover of beams

Fig. 3 Finite element meshing layout of beam-column elements

Table 3 The value of masses for all various frames

Masses (Ton)		
Story ID	2D	3D
3	202.5	1012.5
6	405	2025
9	540	2700

4.1 Material properties

In order to achieve the exact results compared to 3D models, assumptions for materials, members and sections are considered. Concrete02 (uniaxial concrete material object with tensile strength and linear tension softening) and Steel02 (a uniaxial Giuffre-Menegotto-Pinto steel material object with isotropic strain hardening) models are used to predict the behavior of concrete and steel materials in OpenSees software (Menegotto *et al*. 1973). In addition, Steel02 is used to model SMAs material. The Concrete02 model is used to simulate concrete behavior with tensile strength and liner tension softening. The stress-strain curve and model of cyclic behavior are shown in Figs. 4(a)-(b). The parameters used in the Fig. 4(a) are illustrates in Table 4. The Steel02 model is used to predict a uniaxial Giuffre-Menegotto-Pinto steel material object with isotropic strain hardening (Manegotta *et al*. 1973). The stress-strain curve

Table 4 Description of parameters used for Concrete02 model

Parameters	Descriptions
$matTag	Unique material object integer tag
$fpc	Compressive strength*
$epsc0	Strain at compressive strength*
$fpcu	Crushing strength*
$epsU	Strain at crushing strength*
$lambda	Ratio between unloading slope at $epscu and initial slope
$ft	Tensile strength
$Ets	Tension softening stiffness (absolute value) (slope of the linear tension softening branch)

*Note: Compressive concrete parameters should be input as negative values

and model of cyclic behavior are shown in Figs. 5(a)-(b).

Fig. 6 shows the superelastic model used in OpenSees software where SMA has been subjected to multiple stress cycles at a constant temperature and undergoes stress induced austenite–martensite transformation. The behavior of shape memory alloys is symmetric. Therefore, behavior of SMAs is the same in tension and compression. This model used to simulate the behavior of SMAs was proposed by Fugazza (2003) which is modified version introduced by Auricchio and Sacco (1997). The advantages of this model

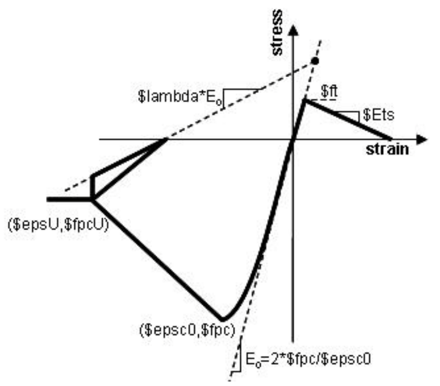

(a) Stress-strain curve

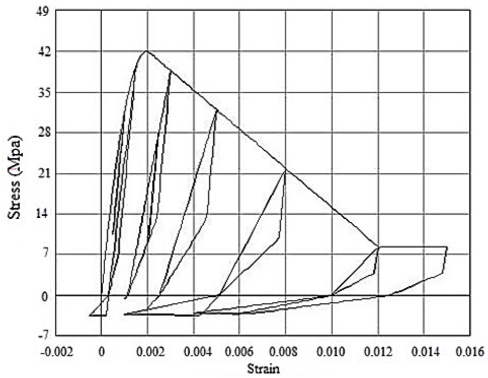

(b) Cyclic behavior

Fig.4 The Concrete02 model (Mazzoni *et al*. 2007)

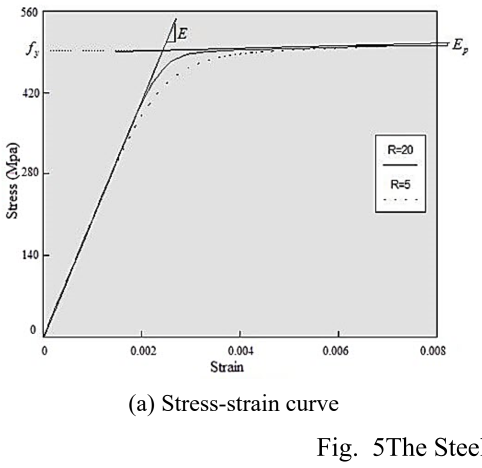

(a) Stress-strain curve

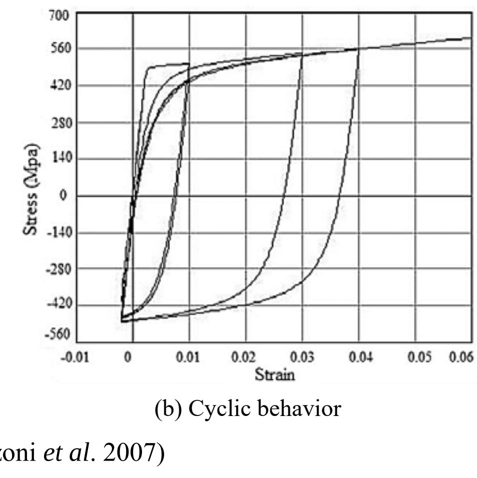

(b) Cyclic behavior

Fig. 5The Steel02 model (Mazzoni *et al*. 2007)

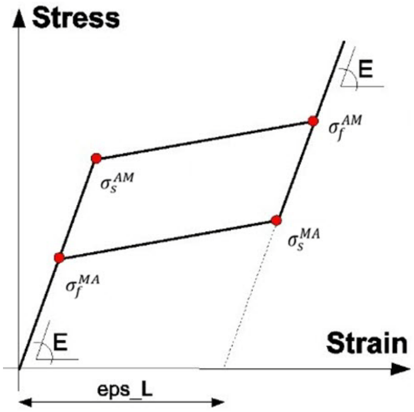

Fig. 6 The stress-strain curve for SMAs used in OpenSees

Table 5 Fundamental periods of models

Story ID	Structure type	Main period (Sec)	
		3D model (Original)	2D model (Validation)
3	Steel	0.39	0.4
	Steel-SMA	0.41	0.42
	SMA	0.42	0.44
6	Steel	0.67	0.66
	Steel-SMA	0.7	0.68
	SMA	0.74	0.72
8	Steel	0.86	0.85
	Steel-SMA	0.93	0.89
	SMA	1	0.96

are simplicity, limited number of the required parameters and showing the partial and complete phase transformations. The main disadvantage is the lack of considerations for speed of loading and temperature in the model. This one-dimensional model describes the behavior of superelastic materials under the desired seismic loadings in terms of several hysteresis loops within a main loop (complete phase transformation). Another assumption used in this model is the consideration of identical elastic modules for austenite and martensite phases.

The parameters used to define the SMAs model are$\sigma_s^{AM}, \sigma_f^{AM}, \sigma_s^{MA}$ *and* σ_f^{MA} (phase transformation stresses), E (modulus of elasticity in the austenite and martensite phases, ε_L (superelastic plateau strain length or maximum residual strain).

4.2 Verification of 2D models

Table 5 represents the comparison of fundamental periods of 3D structures (original model) and 2D models (validation). As shown in Table 5, the negligible difference between main periods results from the verification of 2D frames used in this research and correct mass distribution from 3D model to 2D model in OpenSees software. The results show that the use of SMA as reinforcement in beam increases the fundamental period of the structure compared to steel because of SMA's lower modulus of elasticity than that of steel. In addition, the fundamental periods greatly increase by adding number of stories.

5. Incremental dynamic analyses

Incremental dynamic analysis (IDA) was first proposed by Cornell at Stanford University, and was investigate for a 20-story building during the Vamvatsikos's Ph.D. Thesis (2002a). This is a nonlinear dynamic analysis method that can be used to determine the amount of damage in terms of imposed earthquake intensity. In order to perform the actual dynamic analyses needed for IDA, each appropriate ground motion records must be scaled to cover the entire range of structural response, from elasticity, to yielding, and finally global dynamic instability. Intensity Measure (IM, e.g., peak ground acceleration or the 5%-damped first-mode spectral acceleration $S_a(T_1,\ 5\%)$) and Damage Measure (DM, e.g., peak roof drift or maximum peak inter-story drift $\theta_{\max}$) are two important parameters which must be chosen accurately to generate IDA curves of the structural response. Additionally, performance limit states (e.g., Immediate Occupancy or Collapse Prevention) can be defined on each IDA curve and summarized to produce the probability of exceeding a specified perfor-mance limit state given the IM level (Vamvatsikos *et al*. 2002a).

In this paper, the first mode spectral acceleration ($S_a\ (T_1)$) is used as the IM level, and the peak inter-story drift $\theta_{\max}$ is selected as the DM level. In addition, Immediate Occupancy (IO), Life Safety (LS) and Collapse Prevention (CP) are considered as performance limit states. Thus, $\theta_{\max}$ of 0.001, 0.02 and 0.04 as limit-points corresponding to the IO, LS and CP limit states are selected based on FEMA356, respectively. Therefore, nine structural models including 3-, 6- and 8-story frames with various reinforcement pattern in beams which discussed earlier are considered, and IDAs have been conducted under ten selected ground motion records. Then, IDA curves of the structural response of each frame are obtained and summarized. Finally, determining the performance limit states corresponding to performance levels result in obtaining the capacity of structures (S_a), and nine fragility curves for are presented.

5.1 Ground motions

Incremental Dynamic Analyses (IDA) are performed under ten earthquake records which are all associated with soli type II in terms of shear wave velocity. Table 6 represents ground motion characteristics used for analyses. In order to cover the entire range of structural response and achieving enough accuracy, suitable scaling method must be used. The task is made significantly easier by using an advanced algorithm, like hunt and fill (Vamvatsikos *et al*. 2002b). In this method, the first step is to scale the IM. Thus, a very small amount (0.005 g) is selected as IM ($S_a\ (T_1)$) to ensure the linear response of structure. Then, according to the Eq. (2), IM increases exponentially at each step to find the range of $S_a\ (T_1)$ in which the specific failure occurred. The coefficient of α is equal to 0.05.

Table 6 Ground motions used for analyses

No.	Earthquake	Station	Soil type	PGA(g)
1	Chi-Chi, Taiwan, 1999	CHY080	II	0.902
2	Coyote Lake, 1979	Gilroy Array 3	II	0.434
3	Kobe, 1995	KJMA	II	0.821
4	Landers, 1992	Coolwater	II	0.417
5	Loma Prieta, 1989	Corralitos	II	0.644
6	Morgan Hill, 1984	Anderson Dam	II	0.423
7	N. Palm Springs, 1986	N. Palm Springe	II	0.694
8	Northridge, 1994	Santa Monica	II	0.883
9	Bam, 2003	Bam	II	0.767
10	Tabas, 1978	9101 Tabas	II	0.917

Finally, the scale factor (SF_i) is calculated at each step by using Eq. (3), and is multiplied in earthquake records, where $S_a\,(T_1)$ is the first mode spectral acceleration resulting from unscaled earthquake record. The nonlinear dynamic analyses are conducted by new scaled records.

$$S_a(T_1) = S_a(T_1)_{i-1} + \alpha \times (i-1) \tag{2}$$

$$SF_i = \frac{S_a(T_1)_i}{S_a(T_1)} \tag{3}$$

6. Results

After conducting IDAs under ten different ground motion records and subsequently defining the performance limit state capacities, a large amount of data can be produced. Due to the large number of date curved which represent a specific behavior of the structure, it would be essential to summarize such data in terms of quantity of randomness introduced by the records to achieve a general behavior of the structure. This summarization is possible through statistical methods, and the capacity of buildings can be evaluated more noticeably. Consequently, three statistical percentile values of the 16%, 50% and 84% of DM and IM for each performance limit state have been chosen. Finally, the median values for each IDA curve including Steel, Steel-SMA and SMA corresponding with 3-, 6- and 8-story frames are obtained. Fig. 7 represents the median values of IDA curves for various frames in term of height and reinforcement details. In buildings, the inter-story drift ratio (IDR) is defined as the difference of displacements of the floors above and below the story of interest normalized by the inter-story height. As shown in Fig. 7, the capacity (S_a) is almost identical in 3-story frames. However, in 6- and 8-story frames, the capacity of frame equipped with steel bars are more than other type of frames. Therefore, the use of SMA bars in the plastic hinge regions or all regions of beams would result in the decrease of structure stiffness.

6.1 Failure analysis and fragility curves

In order to extract the probability of the performance limit state occurrence from outputs of IDAs, the graphs known as the fragility curves are utilized. The fragility curves represent the relation between structural damages and selected earthquake intensity. The probabilistic seismic performance is measured by fragility curves, that is, the

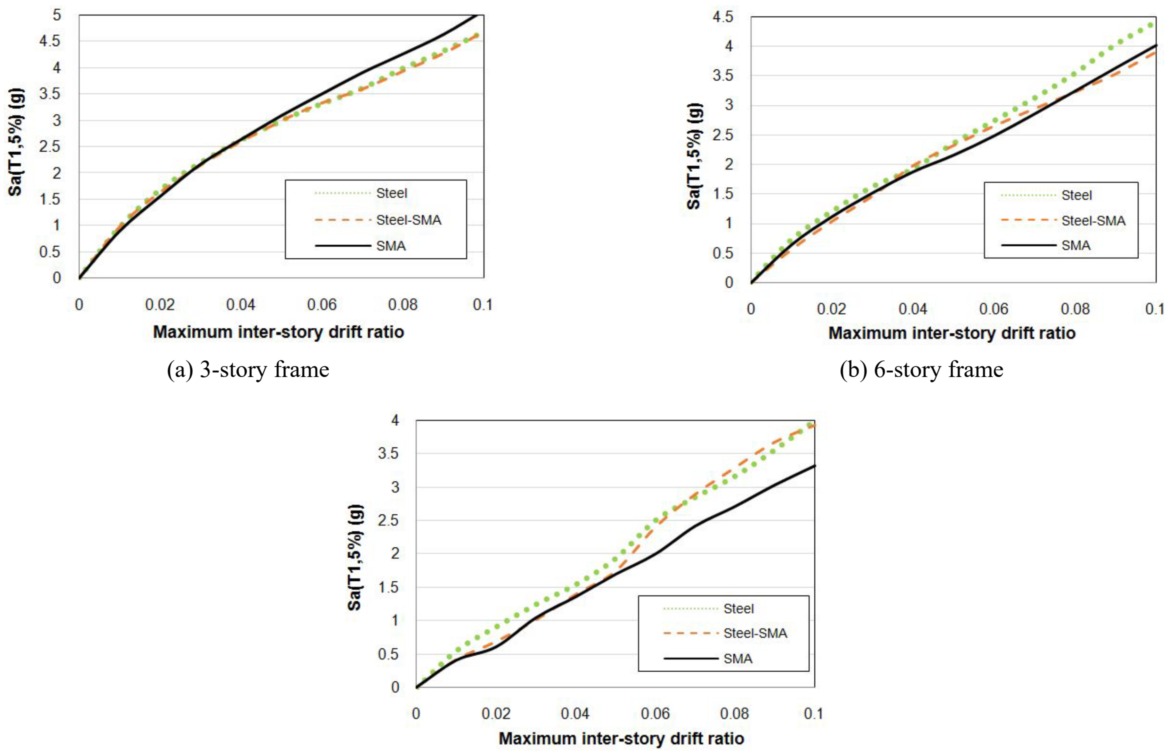

(a) 3-story frame

(b) 6-story frame

(c) 8-story frame

Fig. 7 Median values of IDA curves for various frames

Table 7 Parameters of lognormal distribution function

Story ID	Structure type	Performance level					
		IO	LS	CP	IO	LS	CP
		λ	β	λ	β	λ	β
1	Steel	-0.064	0.288	0.440	0.425	0.878	0.458
	Steel-SMA	-0.050	0.263	0.435	0.370	0.874	0.449
	SMA	-0.139	0.255	0.373	0.398	0.875	0.484
2	Steel	-0.333	0.335	0.206	0.338	0.768	0.195
	Steel-SMA	-0.515	0.338	0.071	0.281	0.704	0.224
	SMA	-0.342	0.346	0.209	0.321	0.757	0.287
3	Steel	-0.587	0.301	-0.043	0.394	0.517	0.417
	Steel-SMA	-0.779	0.321	-0.256	0.371	0.367	0.397
	SMA	-0.831	0.322	-0.320	0.361	0.317	0.397

value of Dsi determines the probability of a specific failure modes occurrence in a specific spectral acceleration ($S_a(T_1)$), where ϕ is cumulative normal distribution function, X is spectral acceleration that has lognormal distribution, and λ, β are mean and standard deviation of Ln(X), respectively.

$$P\left(DS \geq Dsi\, S_a(T_1)\right) = \phi\left(\frac{Ln(X) -\lambda\beta}{}\right) \tag{4}$$

The values of spectral acceleration for various studied frames in all performance levels including IO, LS and CP are shown in Table 6. In addition, Table 7 represents parameters of lognormal distribution function for various frames levels corresponding with performance levels.

Figs. 8 and 9 represent fragility curves in performance limit states including IO, LS and CP for three various reinforcement details corresponding with 3- and 6- story frames. As shown in Fig. 8, the probability of failure in 3-story frame equipped with SMA bars in IO, LS and CP limit states are higher than the other two types. However, this difference is reduced in the IO limit state, and the fragility curves are almost the same in CP limit state. As shown in Fig. 9, the probability of failure in 6-story frame equipped with SMA-Steel bars in all performance limit states are higher than the other two types. Also, the performance of frames is approximately similar in CP limit state. Table 8 represents the values of S_a (capacity of structures) corresponding with failure possibilities of 16%, 50% and84% for three performance levels including IO, LS and CP. As shown in Table 8, by increasing the frames height,

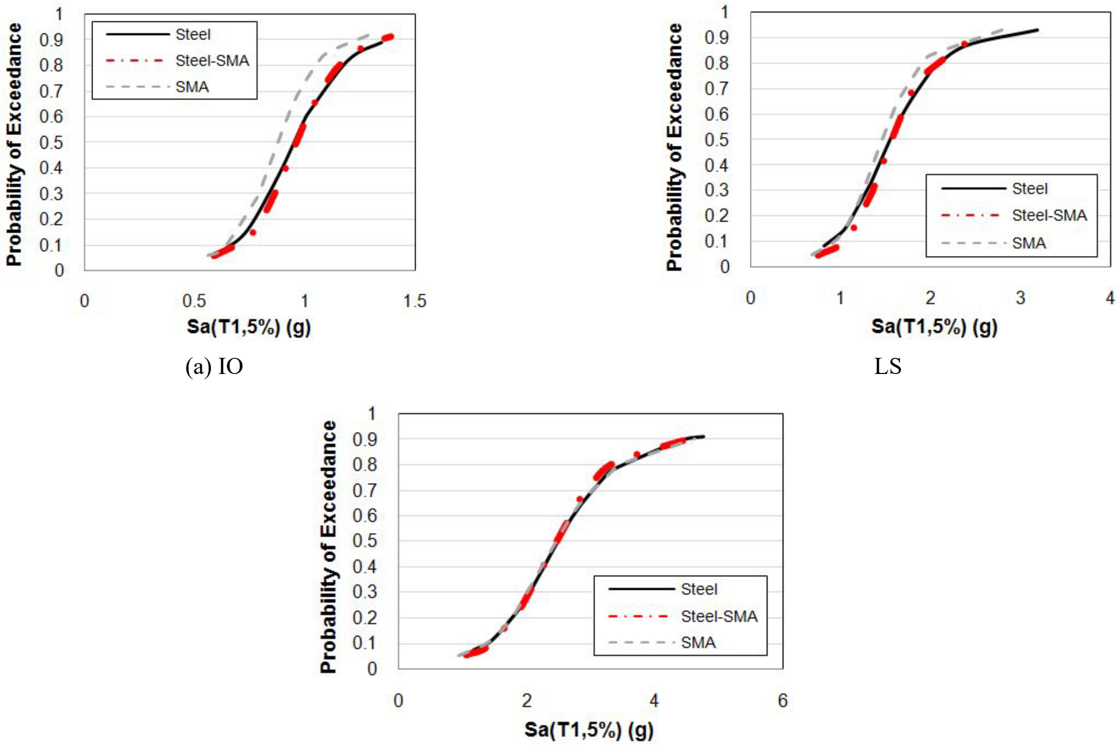

Fig. 8 Fragility curves in various performance limit states for 3-story frames

probability of system failure as a function of earthquake consequences of system damage and failure, and system probability of failure (Korkmaz 2008). The structural fragility for a specified performance limit state is defined as the conditional probability of exceeding the limit state capacity for a given level of ground motion intensity (conditional probability of failure in short). The Fragility curves are drawn utilizing the normal distribution. In this study, fragility curves are drawn base on spectral accelera-tion in structural period, and modelled by two-parameter lognormal distribution function. As shown in Eq. (4) the

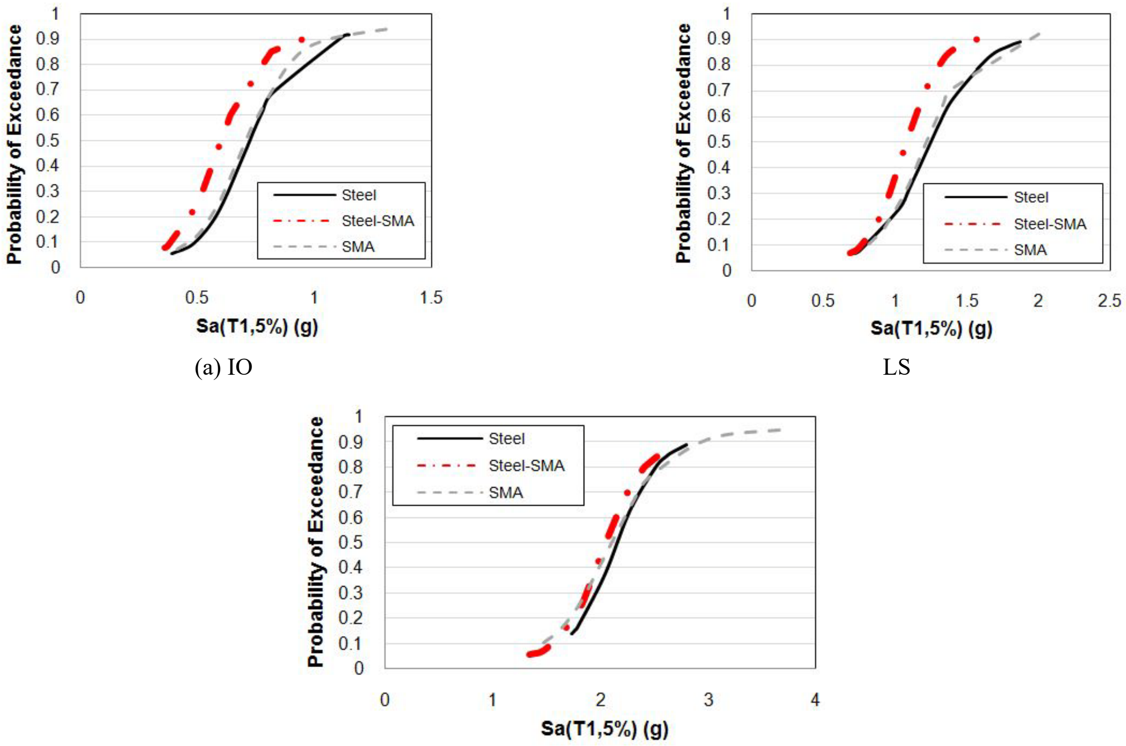

(a) IO

LS

(c) CP

Fig. 9 Fragility curves in various performance limit states for 6-story frames

the possibility of collapse or failure to meet performance levels (IO, LS and CP) in a constant level of seismic intensity increases. Table 9 shows the values of S_a corresponding with failure possibility of 50% for CP limit state which is known as capacity of structure. As shown in Table 9, the capacity reduction of 3-story frames equipped with Steel-SMA and SMA bars compared to Steel bars are 0.3% and 0.4%, respectively. The capacity reduction of 6-story frames equipped with Steel-SMA and SMA bars compared to Steel bars are 2.3% and 5%, respectively, and these reductions for 8-story frames are 13.4% and 17.8%, respectively. According to the previous results, the use of SMA bars in the plastic hinge beams (Steel-SMA) with respect to its use in all beams length (SMA), leads to a reduction in decreased capacity (S_a). In addition, it can be concluded that the decrease in the capacity of frames which equipped with SMA bars can be highlighted by increasing the stories. The capacity (S_a) of frames equipped with SMA and Steel-SMA bars are less than frames with Steel bars. This is due to the lower stiffness of these frames compared to frames with steel bars which results in more displacement during the earthquake. Therefore, the stiffness of frames equipped with SMA and Steel-SMA bars should be increased in order decrease the displacement.

7. Conclusions

In this paper, the use of SMAs as reinforcement in reinforced concrete buildings was investigated. To did this, three different reinforcement details were considered: (1) steel reinforcement (steel) only; (2) SMA bar used in the plastic hinge region of the beams and steel bar in other regions (Steel-SMA); and (3), beams fully reinforced with SMA bar (SMA) and steel bar in other regions. Then, different 2D concrete frames in term of height and reinforcement details were selected from the predefined 3D model. Incremental dynamic analyses (IDA) were performed to determine seismic behavior of various reinforcement details in frames. In addition, Fragility curves for performance levels of concrete frames base on FEMA356 were obtained. The results are presented in the following:

- The use of SMA bars as reinforcements in the plastic hinge beam can improve the ability of some members to recover their own shape after the earthquake. This characteristic of SMA bars results in lower damages in reinforced concrete members and joint during the earthquake, and reduces the cost of repair after the seismic events.
- Due to the lower modulus of elasticity and smaller hysteresis loop in SMA bars compared with Steel bars, the use of SMA bars as reinforcement in concrete structures causes important changes in structural responses. Therefore, these changes must be considered precisely in design processes.
- The value of S_a in Steel-SMA frames are higher than SMA frames, and its recovery capacity is almost similar with SMA frames. However, the SMAs materials are expensive, and the use of Steel-SMA frames can be reasonably effective in seismic zones. The comparison between frames with various reinforcements details shows that S_a of 3-story frames with various reinforcements are almost

Table 8 The values of S_a corresponding with failure possibilities of 16%, 50% and 84%

Story ID	Structure type	$(S_a(T_1,5\%))_{IO}$ (g)		
		16%	50%	84%
3	Steel	0.735	0.947	1.234
	Steel-SMA	0.698	0.958	1.215
	SMA	0.685	0.875	1.089
6	Steel	0.569	0.723	1.025
	Steel-SMA	0.430	0.600	0.808
	SMA	0.522	0.705	0.951
8	Steel	0.415	0.567	0.754
	Steel-SMA	0.335	0.459	0.604
	SMA	0.319	0.434	0.576
		$(S_a(T_1,5\%))_{LS}$ (g)		
3	Steel	1.062	1.553	2.279
	Steel-SMA	1.136	1.566	2.241
	SMA	1.049	1.465	2.051
6	Steel	0.891	1.245	1.685
	Steel-SMA	0.832	1.076	1.375
	SMA	0.918	1.216	1.733
8	Steel	0.657	0.964	1.333
	Steel-SMA	0.549	0.769	1.094
	SMA	0.514	0.721	1.017
		$(S_a(T_1,5\%))_{CP}$ (g)		
3	Steel	1.577	2.471	3.77
	Steel-SMA	1.628	2.463	3.766
	SMA	1.610	2.460	3.901
6	Steel	1.783	2.157	2.598
	Steel-SMA	1.661	2.049	2.519
	SMA	1.636	2.107	2.742
8	Steel	1.169	1.687	2.474
	Steel-SMA	1.016	1.461	2.122
	SMA	0.965	1.387	1.967

identical. but, in 6- and 8-story frames, S_a of Steel frames are higher than others. In other words, frames with SMA bars in the all length or plastic hinge region of the beam have reached a same level of seismic demand under lower spectral acceleration which can be resulted from the decreased stiffness caused by SMA bars.

The comparison between fragility curves show that the exceeding probability of frames from each performance limit states (IO, LS and CP) increases for a certain spectral acceleration by increasing the height of structure. The large residual displacements are one of the main reasons of costly retrofit of structures and bridges against seismic events. SMAs are the only material that can recover the most inelastic displacements. The use of SMA bars in the beam-column elements or plastic hinge region of beams results in a major advance in seismic design of structures. This will ultimately lead to structures with more suitable ability in terms of serviceability after strong earthquakes.

Table 9 The values of S_a corresponding with failure possibility of 50% for CP limit state

Structure type	Story ID		
	3	6	8
Steel	2.471	2.157	1.687
Steel-SMA	2.463	2.049	1.461
SMA	2.460	2.107	1.387

References

Abdulridha, A., Palermo, D. and Foo, S. (2010), “Seismic behavior of SMA reinforced concrete beams”, *Proceedings of the 9th US National and 10th Canadian Conference on Earthquake Engineering: Reaching Beyond Borders*, Toronto, Canada, July.

Alam, M.S., Youssef, M.A. and Nehdi, M. (2007), “Seismic behavior of concrete beam-column joints reinforced with super-elastic shape memory alloys”, *Proceedings of the 9th Canadian Conference on Earthquake Engineering*, Ottawa, Canada, June, Paper No.1125, p. 10.

Alam, M.S., Youssef, M.A. and Nehdi, M. (2008), “Analytical prediction of the seismic behavior of superelastic shape memory alloy reinforced concrete elements”, *Eng. Struct.*, **30**(12), 3399-3411.

Alam, M.S., Nehdi, M. and Maged, A.Y. (2009), “Seismic performance of concrete frame structures reinforced with superelastic shape memory alloys”, *Smart Struct. Syst.*, *Int. J.*, **5**(5), 565-585.

Alam, M.S., Moni, M. and Tesfamariam, S. (2012), “Seismic over-strength and ductility of concrete buildings reinforced with superelastic shape memory alloy bar”, *Eng. Struct.*, **34**(2012), 8-20.

Alvandi, S. and Ghassemieh, M. (2014), “Application of shape memory alloys in seismic isolation”, *Civil Eng. Infrastruct. J.*, **47**(2), 153-171. ISSN: 2322-2093

Andrawes, B. and DesRoches, R. (2007), “Effect of hysteretic properties of superelastic shape memory alloys on the seismic performance of structures”, *Struct. Control Health Monitor.*, **14**(2), 301-320.

Anson, T. (1999), “Shape memory alloys - Medical applications”, *Mater. World*, **7**(12), 745-747.

Auricchio, F. and Sacco, E. (1997), “A one-dimensional model for superelastic shape-memory alloys with different elastic properties between austenite and martensite”, *Int. J. Non-Linear Mech.*, **32**(6), 1101-1114.

CSA A23.3-04 (2004), Design of Concrete Structures; (5th Ed.), Canadian Standards Association, Rexdale, ON, Canada.

Dolce, M. and Cardone, D. (2001), “Mechanical behaviour of shape memory alloys for seismic applications1. Martensite and austenite NiTi bars subjected to torsion”, *Int. J. Mech. Sci.*, **43**(11), 2631-2656.

Dolce, M. and Cardone, D. (2001), “Mechanical behaviour of shape memory alloys for seismic applications 2. Austenite NiTi wires subjected to tension”, *Int. J. Mech. Sci.*, **43**(11), 2657-2677.

FEMA (2000), Recommended seismic design criteria for new steel moment-frame buildings; Report No. FEMA-350, SAC Joint Venture, Federal Emergency Management Agency, Washington DC, USA.

Fugazza, D. (2003), “Shape-memory alloy devices in earthquake engineering: mechanical properties, constitutive modelling and numerical simulations”, Master’s Thesis; European School for Advanced Studies in Reduction of Seismic Risk (ROSE School), Pavia, Italy.

Jalayer, F. and Cornell, C.A. (2003), “A technical framework for probability-based demand and capacity factor design”, Pacific Earthquake Engineering Research Center PEER Rep. 2003/8, PEER Berkeley, CA, USA.

Khaloo, A.R., Eshghi, I. and Piran Aghl, P. (2010), “Study of behavior of reinforced concrete beams with smart bars using finite element modeling”, *Int. J. Civil Eng.*, **8**(3), 221-231.

Korkmaz, K.A. (2008), “Evaluation of seismic fragility analyses”, *Proceedings of the 14th World Conference on Earthquake Engineering*, Beijing, China, October.

Mazzoni, S., McKenna, F., Scott, M.H. and Fenves, G.L. (2007), “OpenSees Command Language Manual”, Pacific Earthquake Engineering Research Center; University of California, Berkeley, CA, USA.

Menegotto, M. and Pinto, P.E. (1973) “Method of analysis of cyclically loaded RC plane frames including changes in geometry and non-elastic behavior of elements under normal force and bending”, Preliminary Report IABSE; Volume 13.

Mo, Y.I., Song, G. and Otero, K. (2004), “Development and testing of a proof-of-concept smart concrete structures”, *Proceeding of Smart Structures Technologies and Earthquake Engineering*, Osaka, Japan, July.

Motahari, S.A., Ghassemieh, M. and Abolmaali, S.A. (2007), “Implementation of shape memory alloy dampers for passive control of structures subjected to seismic excitations”, *J. Construct. Steel Res.*, **63**(12), 1570-1579.

NBCC (2005), National Building Code of Canada; Canadian Commission on Building and Fire Codes, National Research Council of Canada, Ottawa, Canada.

Ocel, J., DesRoches, R., Leon, R.T., Hess, W.G., Krumme, R., Hayes, J.R. and Sweeney, S. (2004), “Steel beam-column connections using shape memory alloys”, *J. Struct. Eng.*, **130**(5), 732-740.

Omar, M. (2011), “Analytical prediction of seismic response of steel frames with superelastic shape memory alloy”, *Proceedings of International Conference on Earthquake and Structural Engineering*, Venice, Italy, November.

Paulay, T. and Priestley, M.N.J. (1992), *Seismic Design of Reinforced Concrete and Masonry Buildings*, John Wiley and Sons, Inc., New York, NY, USA.

Srinivasan, A.V. and McFarland, M.D. (2001), *Smart Structures – Analysis and Design*, Cambridge University Press.

Varela, S. and Saiidi, M. (2014), “Dynamic performance of novel bridge columns with superelastic CuAlMn shape memory alloy and ECC”, *Int. J. Bridge Eng. (IJBE)*, **2**(3), 29-58.

Vamvatsikos, D. and Cornell, C.A. (2002a), “Incremental dynamic analysis”, *Earthq. Eng. Struct. Dyn.*, **31**(3), 491-514.

Vamvatsikos, D. and Cornell, C.A. (2002b), “The incremental dynamic analysis and its application to performance-based earthquake engineering”, *Proceedings of the 12th European Conference on Earthquake Engineering*, Barbican Centre, London, UK, September.

CC